

Single-Pulse Preparation of the Uniform Superpositional State used in Quantum Algorithms

G.P. Berman¹, F. Borgonovi^{2,3}, F.M. Izrailev⁴, and V.I. Tsifrinovich⁵

¹*T-13 and CNLS, Los Alamos National Laboratory, Los Alamos, New Mexico 87545*

²*Dipartimento di Matematica e Fisica, Università Cattolica, via Musei 41, 25121 Brescia, Italy*

³*I.N.F.N., Sezione di Pavia and I.N.F.M., Gruppo Collegato di Brescia*

⁴*Instituto de Fisica, Universidad Autonoma de Puebla, Apdo. Postal J-48, Puebla 72570, Mexico*

⁵*IDS Department, Polytechnic University, Six Metrotech Center, Brooklyn NY 11201*

We examine a single-pulse preparation of the uniform superpositional wave function, which includes all basis states, in a spin quantum computer. The effective energy spectrum and the errors generated by this pulse are studied in detail. We show that, in spite of the finite width of the energy spectrum bands, amplitude and phase errors can be made reasonably small.

1. Both the Shor and the Grover quantum algorithms begin with the preparation of a uniform superposition of the basis states. In Shor's algorithm, it is a superposition in the x -register for the modular exponentiation: $a^x \pmod{N}$. For Grover's algorithm, it is a superposition of all possible entries of the unsorted data. In the language of computer science, the transformation of the ground state of the L -qubit register,

$$|0_{L-1}0_{L-2}\dots0_10_0\rangle, \quad (1)$$

into the uniform superposition of all possible basic states,

$$\Psi_{unif} = \frac{1}{2^{L/2}} \sum |n_{L-1}n_{L-2}\dots n_1n_0\rangle, \quad (n_k = 0, 1), \quad (2)$$

is provided by the Hadamard transformation [1]. In physical systems, this transformation can be implemented, for example, using two different methods: 1) by a selected $\pi/2$ -pulse excitation of each qubit, and 2) by non-selective excitation of all qubits using a single $\pi/2$ -pulse. The first method could be used, for example, for a chain of spins connected by the Ising interaction. Unfortunately, in this case non-resonant effects disturb the uniform superposition. The reason is that a $\pi/2$ -pulse acts not only on the chosen resonant spin but also on all other spins [2]. Besides, this method requires the application of L pulses. The second method requires only a single $\pi/2$ -pulse. This method also cannot provide a perfect uniform superposition (2). The second method is used currently in developed statistical ensemble quantum computation [3–5].

In this paper, we analyze the second method. First we discuss the Hamiltonian of the system, then the effective energy spectrum in the rotating reference frame and, finally, the error generated by a $\pi/2$ -pulse. We present the

results of numerical simulation of a chain which includes 10 spins. We show that, in spite of the finite width of the energy spectrum bands, the amplitude and phase errors can be made acceptably small.

2. Consider a chain of spin 1/2 nuclei described by the operators I_k . Assume that these spins have slightly different Larmor frequencies, ω_k and are connected by Ising interactions. In a liquid NMR quantum computation, one utilizes a statistical ensemble of such chains [3–5]. To prepare a uniform superposition (2), a $\pi/2$ -pulse must be polarized along the $(-y)$ -axis of the rotating reference frame (if initially the nuclear spins point in the positive z -direction). The Hamiltonian of the system in the rotating frame is [2],

$$\mathcal{H} = \sum_{k=0}^{L-1} [-(\omega_k - \omega)I_k^z + \Omega I_k^y] - 2J \sum_{k=0}^{L-2} I_k^z I_{k+1}^z, \quad (3)$$

where $\hbar = 1$, Ω is the amplitude of the pulse in the frequency units (the Rabi frequency), ω is the frequency of the pulse, and J is the constant of the Ising interaction. During the action of a $\pi/2$ -pulse, the second term, ΩI_k^y , in the Hamiltonian (3) is the main one, the two other terms are supposed to provide small corrections to the spin dynamics. To choose the values of parameters, we assume that the following inequalities are satisfied for our spin quantum computer,

$$J \ll |\omega_{k+1} - \omega_k|, \quad \Omega \ll \omega_k. \quad (4)$$

Assuming $J/2\pi \sim 0.1\text{kHz}$, $(\omega_{k+1} - \omega_k)/2\pi \sim 1\text{kHz}$, $\omega_k/2\pi \sim 100\text{MHz}$, we shall consider values of $\Omega/2\pi$ up to 10MHz.

3. Next, we shall discuss the effective energy spectrum described by the Hamiltonian (3). To understand the behavior of the energy spectrum, we first analyze a system containing two spins only. When the inhomogeneity and the Ising interaction are absent, the energy spectrum consists of three lines: $E_0 = -\Omega$, $E_1 = 0$, and $E_2 = \Omega$. The first level corresponds to the state, $|00\rangle_{-y}$, where the index “ $-y$ ” indicates that both spins point in the $(-y)$ -direction ($(-y)$ -representation). The twice degenerate level, E_1 , corresponds to the states, $|01\rangle_{-y}$ and $|10\rangle_{-y}$, and the energy level E_2 , refers to the state $|11\rangle_{-y}$. First, we consider the effect of inhomogeneity when the Ising interaction is absent. Assume, for example, that $\omega = \omega_0$

and $\omega_1 = \omega_0 + \Delta\omega$. Then, the effective field for spin “1” in the frequency units is, $\Omega_{eff} = \sqrt{\Omega^2 + \Delta\omega^2}$. The energy levels are given by the expressions,

$$E_0 = -(\Omega + \Omega_{eff})/2, \quad E_1 = (\Omega - \Omega_{eff})/2, \quad (6)$$

$$E'_1 = (\Omega_{eff} - \Omega)/2, \quad E_2 = (\Omega + \Omega_{eff})/2.$$

The main effect is the splitting of the central line into two lines with the energy separation,

$$\Delta E = E' - E \approx (\Delta\omega)^2/2\Omega.$$

Important fact is that this splitting decreases as $1/\Omega$ as Ω increases.

Let us consider the error generated by a non-resonant spin. If the initial state of this spin is $|0\rangle_z$, then with linear accuracy, $\Delta\omega/\Omega$, the wave function of the spin, $\Psi(t)$, can be written as,

$$\Psi(t) = [\cos(\Omega t/2) + i(\Delta\omega/\Omega) \sin(\Omega t/2)]|0\rangle_z + \sin(\Omega t/2)|1\rangle_z.$$

After a $\pi/2$ -pulse ($\Omega t = \pi/2$), we have:

$$\Psi(\pi/2\Omega) \approx \frac{1}{\sqrt{2}} \left(e^{i\Delta\omega/\Omega} |0\rangle_z + |1\rangle_z \right).$$

Thus, in first order in $\Delta\omega/\Omega$, the inhomogeneity generates only a phase error which decreases as $1/\Omega$.

Now, we consider the effect of the Ising interaction when the inhomogeneity is absent. At first sight, the Ising interaction produces an additional “effective field” in the z -direction, and its influence on the energy spectrum must also decrease as Ω increases.

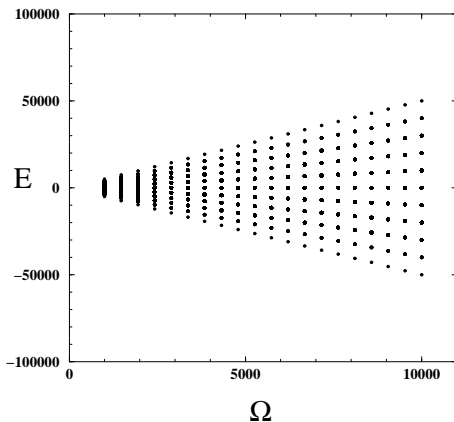


FIG. 1. The energy spectrum as a function of Ω .

However, the “effective field” approach is not correct in this case. It is easy to check that the ground state is $|00\rangle_{-y}$ with a small admixture of the state $|11\rangle_{-y}$. It has the energy, $E_0 = -\sqrt{\Omega^2 + (J/2)^2}$. The central energy splits into two levels $\pm J/2$, which correspond to symmetric and antisymmetric superpositions of the states $|01\rangle_{-y}$

and $|10\rangle_{-y}$, and $E_2 = -E_0$. When the Rabi frequency, Ω , increases, the influence of the Ising interaction on the energy levels, E_0 and E_2 decreases. But the splitting between the central energy levels does not change as Ω increases: $\Delta E_1 = J$. One might expect that this splitting will generate an error which does not decrease as Ω increases. Fortunately, it does not happen. If both spins point initially in the positive z -direction, the wave function, $\Psi(t)$, can be written as,

$$\Psi(t) \approx (1/2)[e^{i\Omega t}|00\rangle_{-y} - e^{-i\Omega t}|11\rangle_{-y} + ie^{iJt/2}(|01\rangle_{-y} + |10\rangle_{-y})],$$

where we neglected the terms $\sim (J/\Omega)^2$. At the end of the $\pi/2$ -pulse, we have,

$$\Psi(\pi/2\Omega) \approx \frac{i}{\sqrt{2}} \left[|00\rangle_{-y} + |11\rangle_{-y} + e^{i\pi J/4\Omega} (|01\rangle_{-y} + |10\rangle_{-y}) \right].$$

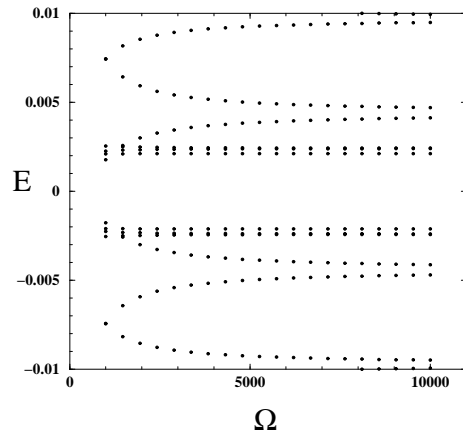


FIG. 2. The structure of a narrow strip of the central band shown in Fig.1.

For $J = 0$, we have a uniform superposition of the basis states (in both $(-y)$ - and z -representations). For $J \neq 0$, to first order in J/Ω , the Ising interaction (similar to the inhomogeneity) generates only a phase error which decreases as $1/\Omega$. The non-vanishing bandwidth, $\Delta E_1 = J$, does not cause a non-vanishing error. This happens because the phase error is proportional to the duration of a $\pi/2$ -pulse which is proportional to $1/\Omega$.

3. Next, we present the results of numerical simulations with $L = 10$ qubits. These simulations require operations on a digital computer in the Hilbert space with dimension $D = 2^{10} = 1024$.

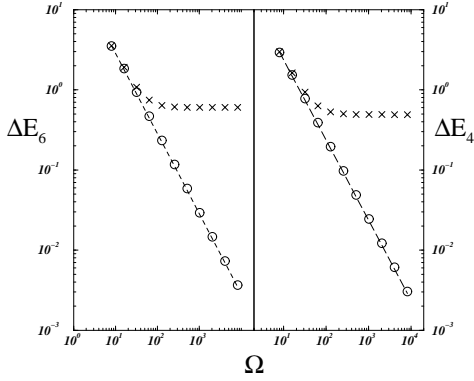


FIG. 3. Widths ΔE_6 , (left) ΔE_4 (right) of the 6th (central) and the 4th band vs Ω . Open circles are for $J = 0$, crosses for $J = 0.1$. Dashed lines are the best fit to A/Ω (circles) where $A = 28.466$ (left) and $A = 23.673$ (right).

If the Ising interaction and the inhomogeneity of the frequencies, ω_k , are both absent, the energy spectrum of the Hamiltonian (3) consists of 11 equidistant levels separated by gaps with value Ω . Both the interaction and the inhomogeneity cause splitting of all inner levels. This leads to formation of energy bands.

Fig. 1 shows the energy spectrum as a function of Ω , for the following values of parameters,

$$\omega_{k+1} - \omega_k = 1, \quad (k = 0, \dots, 9), \quad J = 0.1, \quad \omega_k - \omega = k - 4.5.$$

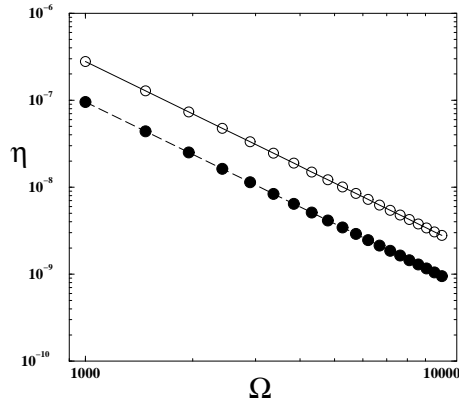


FIG. 4. Dependence on Ω of the maximal (open circles) and average errors (full circles) for the amplitude modulus, $|A_n|$, on Ω . The full line is the best fit, $0.2787/\Omega^2$, while the dashed is $0.0953/\Omega^2$. Other parameters are the same as in Fig.1.

The last equation means that the frequency ω of a $\pi/2$ -pulse is equal to the average Larmor frequency, $\langle \omega_k \rangle = (1/10) \sum_{k=0}^9 \omega_k$. For each Ω , there are 1024 energy levels. At the scale shown in Fig. 1, each band is represented by a point.

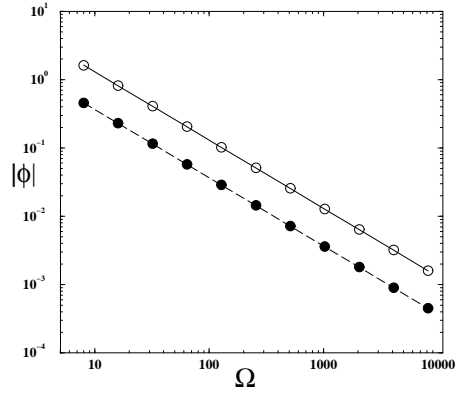


FIG. 5. Dependence of the maximal (open circles) and average errors (full circles) for the phase errors $|\phi_n|$, on Ω . Full line is the best fit $13.0216/\Omega$, while dashed is $3.6606/\Omega$. Other data are the same as in Fig.1.

In fact, each band has a complicated structure. As an example, Fig. 2 shows the structure of a narrow strip of the central band as a function of Ω . Fig. 3 (left) shows the dependence of the width of the central band, ΔE_6 , on Ω (in the logarithmic scale). When the interaction between spins is absent (circles in Fig. 3), ΔE_6 decreases approximately as $1/\Omega$. A finite interaction (crosses in Fig. 3) changes this picture. After the width of the band caused by the inhomogeneity decreases to the value of approximately $6J$ (at $\Omega \approx 50$), its value does not decrease. This dependence of ΔE_6 on Ω is qualitatively similar to the results discussed above for two spins. Fig. 3 (right) shows similar dependence for the the width of the 4th band, ΔE_4 .

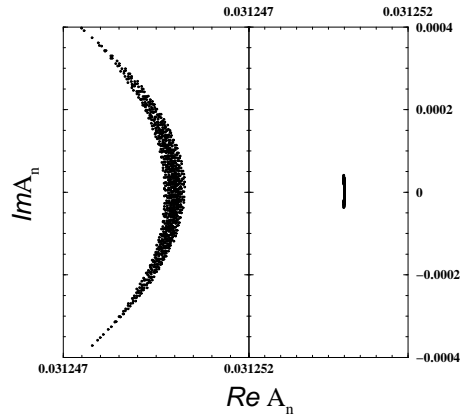


FIG. 6. The distribution of the complex amplitudes, A_n , in the complex plane for $\Omega = 10^3$ (left) and $\Omega = 10^4$ (right). Other parameters are the same as in Fig.1.

Now we consider the errors generated in the process of preparation of a uniform superposition of the basis states, Ψ_{unif} .

In the rotating frame, the spin dynamics can be described as a superposition of stationary solutions with constant coefficients, which can be found from the initial

conditions. In the absence of both the interaction between spins and the inhomogeneity, a $\pi/2$ -pulse applied to the ground state, $|0_{L-1}\dots 0_0\rangle_z$, generates a uniform superposition of all 2^L basic states with the amplitudes $1/\sqrt{2^L}$.

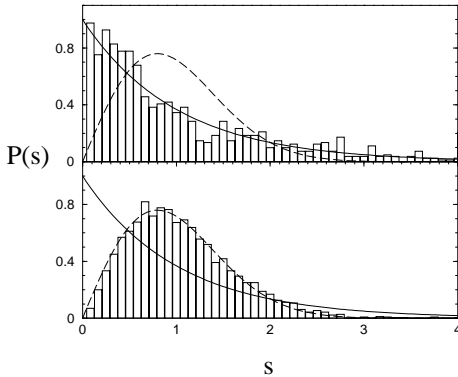


FIG. 7. Level spacing distribution for a system of $L = 12$ spins; $\Omega = 100$; $\omega = \omega_0$, $\omega_k = \omega_0 + k$, $J = 20$ (upper); $J = 100$ (lower). The continuous line shows the Poisson distribution, while the dashed curve shows the GOE distribution.

To describe the error in the complex amplitude, $A_n = |A_n| \exp(i\Phi_n)$, of the state $|n\rangle_z$ ($0 \leq n \leq 2^L - 1$), we use two quantities: 1) $\eta = |2^{-L/2} - |A_n||$ which describes the error of the amplitude modulus, $|A_n|$, and 2) the phase modulus, $|\Phi_n|$, which describes the phase error (as $\Phi_n = 0$ in the ideal case). Fig. 4 shows the dependences of the maximal error, η_{max} and the average error, η_{ave} , on the Rabi frequency, Ω . One can see that both quantities decrease approximately as $1/\Omega^2$. Fig. 5 shows similar dependences of the phase error on Ω . Both, $|\Phi|_{max}$ and $|\Phi|_{ave}$ decrease approximately as $1/\Omega$. This corresponds to the results derived above for two spins. Note that for parameters we chose (which correspond to $J \ll \Delta\omega$), the main contribution to the error depends on the inhomogeneity. The plots presented in Figs 4 and 5 do not change significantly when $J = 0$. Fig. 6 shows the distribution of the complex amplitudes, A_n , in the complex plane for $\Omega = 10^3$ and $\Omega = 10^4$. One can see that the distribution of A_n has a form of the arc whose length and width decrease as Ω increases.

4. In this section, we note that the quantum Hamiltonian (3) belongs to the so-called quantum non-integrable systems. This means that, treated classically, these systems exhibit chaotic behavior for some range of parameters and initial conditions. (See, for example, [6] and references therein.) The quantum properties of classically chaotic systems can be investigated by a detailed analysis of their eigenvalues and eigenfunctions [7]. This analysis will be the subject of future investigation. Here, we concentrate on the statistics of neighboring energy levels spacing, $P(s)$. Indeed it has been conjectured that $P(s)$ for a chaotic system depends only on some general

symmetries [8]. In our case (for Hermitian matrices), we can assume the quantum chaos regime as described by a Wigner-Dyson distribution. Fig. 7 shows the transition of $P(s)$, from the Poisson distribution to the Wigner-Dyson distribution of the Gaussian orthogonal ensemble (GOE) of Hermitian matrices.

As one can see from Fig. 7, the transition to chaos appears for relatively large values of J which are far beyond the range of quantum computation. Also, the appearance of the Poisson distribution, which should be a fingerprint of integrability, appears at relatively high values of J , out of quantum computation regime. Level statistics in the quantum computation regime will be the subject of future investigations.

5. In conclusion, we investigated the errors generated by a single-pulse implementation of the Hadamard transformation for a chain of spins connected by the Ising interaction. In the rotating reference frame, the interaction between spins and the inhomogeneity of the Larmor frequencies split the energy levels into the bands. The characteristic width of the band caused by the inhomogeneity decreases as $1/\Omega$ as the Rabi frequency, Ω , increases. The contribution to the band widths due to the Ising interaction between spins remains constant. In spite of this fact, errors generated in the process of preparation of the uniform wave function decrease monotonically as Ω increases. When the Rabi frequency, Ω , increases, the errors of the amplitude modulus, $|A_n|$, decrease as $1/\Omega^2$. The phase errors decrease only as $1/\Omega$. For reasonable values of Ω , the errors of the amplitude's modulus, $|A_n|$, become negligible. The phase error can be reduced to the order of 10^{-5} rad. Thus, both the errors caused by the inhomogeneity and the interaction between spins can be made reasonably small, for a single-pulse generation of the superpositional wave function used in the main quantum algorithms.

ACKNOWLEDGMENTS

The work of GPB and VIT was supported by the Department of Energy (DOE) under contract W-7405-ENG-36, by the National Security Agency (NSA) and Advanced Research and Development Activity (ARDA). FB acknowledges financial support from INFN and INFM.

[1] A.O. Pittenger, *An Introduction to Quantum Computing Algorithms (Progress in Computer Science and Applied Logic, V. 19)*, Birkhäuser, Boston, 1999.

[2] G.P. Berman, G.D. Doolen, R. Mainieri, V.I. Tsifrinovich,

Introduction to Quantum Computers, World Scientific Publishing Company, 1998.

- [3] D.G. Cory, A.F. Fahmy, T.F. Havel, Proc. Natl. Acad. Sci. USA. 94, 1634 (1997).
- [4] I.L. Chuang, N.A. Gershefeld, M. Kubinec, *Phys. Rev. Lett*, **80**, 3408 (1998).
- [5] N.A. Gershenfeld, I.L. Chuang, *Science*, **275**, 350 (1997).
- [6] L.E. Reichl, *The Transition to Chaos*, Springer-Verlag, 1992.
- [7] F.M.Izrailev, Phys. Rep. **196**, 299 (1990)
- [8] O.Bohigas, in Proceedings of the 1898 Les Houches Summer School *Chaos and Quantum Physics*, eds M.J.Giannoni, A.Voros, J.Zinn-Justin (Elsevier Science Publisher B.V. North-Holland, Amsterdam, 1991), p.89